

Enhanced Diradical Nature in Oxyallyl Derivatives Leads to Near Infra Red Absorption: A Comparative Study of the Squaraine and Croconate Dyes Using Computational Techniques[†]

Kola Srinivas,^{‡,§} Ch. Prabhakar,^{‡,§} C. Lavanya Devi,^{‡,§} K. Yesudas,[‡] K. Bhanuprakash,^{*,‡} and V. Jayathirtha Rao^{*,§}

Inorganic Chemistry Division and Organic Chemistry Division, Indian Institute of Chemical Technology, Hyderabad 500 007, India

Received: November 9, 2006; In Final Form: February 20, 2007

We apply many criteria to estimate the diradical character of the ground state singlets of several oxyallyl derivatives. This is carried out as the oxyallyl derivatives like squaraine and croconate dyes can be represented by both mesoionic and diradical formulas, the domination of which would characterize its lowest energy transition. One criterion applied is the singlet–triplet gap, which is known to be inversely proportional to the diradical character. Another criterion is the occupation number; this is determined for the symmetry broken state of the molecules in the unrestricted formalism, and the difference of occupation in the HOMO and LUMO is related to the diradical character. The diradical character of all of the croconates and few squaraines is estimated to be large. All of these have absorption above 750 nm and can be classified as near infrared (NIR) dyes, leading to the inference that NIR absorptions in these molecules are largely due to the dominance of the diradical character. To understand the reliability of the DFT methods for the absorption property predictions of these molecules, TD–DFT studies to calculate the vertical excitation energies have been carried out, using the B3LYP/ BLYP exchange correlation functionals and the LB94 asymptotic functional with and without the inclusion of solvent. The deviations, in both the squaraine series (average lower diradical character), are found to be systematic, and with the inclusion of the solvent in the calculation, the deviations decrease. The best least-squares fit with the experimentally observed values using B3LYP/6-311G(d, p) for the symmetric squaraines yields an *R* value of 0.92 and, for the unsymmetric squaraines, an *R* value of 0.936. With inclusion of the solvent, the *R* value is 0.96 for the symmetric squaraines and 0.961 for the unsymmetric squaraines, indicating that these DFT functionals with linear scaling may be used to study these systems. The croconate dyes, however, have larger deviation from the experimentally observed values in all of the functionals studied even after inclusion of the solvent effects. The deviations are also not systematic. The deviation with respect to the experiment in this case is attributed to the average larger diradical character in this series.

Introduction

Organic “functional” dyes with intense electronic absorption in the near-infrared region (NIR) are of interest in current research as they are useful in medicine, semiconductors, telecommunications, solar cells, etc.^{1–5} Interest in organic functional dyes is due to the combination of features like flexibility and high interaction with light, and over and above all these is the custom tailored synthesis of the dye in the absorption range of our choice. Here computational techniques based on quantum chemical theories, which are replacing the earlier empirical rules, are playing a major role in understanding the dyes post eriori experiment or in suggesting modifications, a priori synthesis suitable to the applications. Some promising NIR dyes are the symmetrical squaraine (a in Chart 1 with $R = R'$), unsymmetrical squaraine (a in Chart 1 with $R \neq R'$), and croconate dyes (b in Chart 1) all of which contain the oxyallyl substructure (c in Chart 1). These are known to exhibit intense π – π^* transitions. Some earlier reports have classified

the transitions in these molecules as (donor–acceptor) charge-transfer transitions.⁶ Recently, we carried out high level SAC-CI studies of some of these molecules and found that these have very little charge transfer and more charge rearrangement in the low-energy transitions.⁷ The electronic structures of these can be understood from the resonance structure contributions from both the mesoionic and the diradical form as shown in Scheme 1 for a simple croconate dye.^{1b,8} Depending on the geometry and substitutions, the structure can be stabilized either in the mesoionic or the diradical form.

Understanding and prediction of properties of these molecules using SAC-CI methodologies can be carried out successfully as shown by the earlier studies.⁷ However, these calculations are time-consuming and not suited for routine prediction. TD–DFT is being suggested as a method of choice for routine prediction of the absorption maxima for many colorants and dyes in spite of the approximation of the exchange-correlation functional by the time independent exchange correlation functional, which is known as the adiabatic approximation.^{9–12} This is attributed to its good performance both from the computation time involved and reasonably good accuracy in prediction of the excitation energies. It has been applied to many conjugated dyes, which show large absorptions in the visible region, and

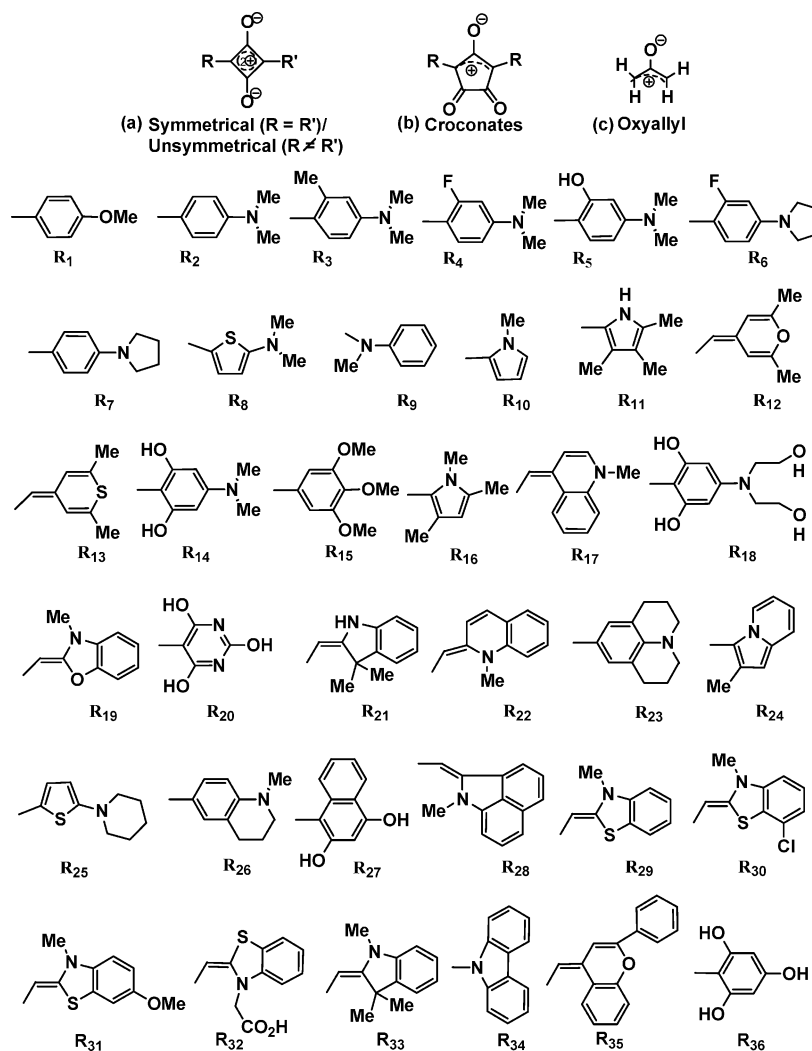
* To whom correspondence should be addressed. E-mail: bhanu2505@yahoo.co.in.

[†] ICT communication number 070326.

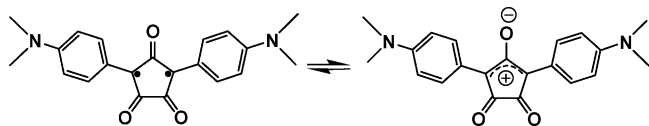
[‡] Inorganic Chemistry Division.

[§] Organic Chemistry Division.

CHART 1: Structures of the Molecules Studied in This Work



SCHEME 1: Resonance Structures of a Croconate Dye: Diradical Form and Mesoionic Form



its performance is judged.^{9–12} If the resonance structure shown in Scheme 1 is dominated by the mesoionic form (diradical character is not very large), we could make use of standard DFT methodologies for the property prediction. In an earlier report, using B3LYP/6-31+G(d) for a TD-DFT study of an oxyallyl derivative (absorption maxima 575 nm) with two sulfur atoms in the ring, Fabian obtained a calculated value that is quite close to the experimentally determined value with a small deviation of only 10 nm.⁸ It was suggested by the author that the resonance structure is probably dominated in their case by the mesoionic formula. Other than this, we have not come across any systematic study of these molecules, using the TD-DFT methodologies.

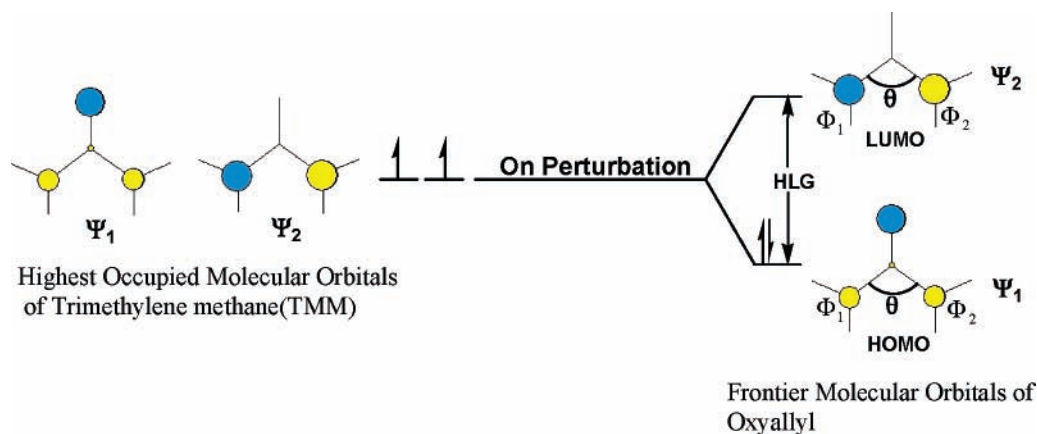
To understand the reliability of the single determinant methods like the TD-DFT for estimation of the transition energies, we first have to estimate the diradical character in these molecules. We have divided the oxyallyl molecules into three series, namely the symmetrical and unsymmetrical squaraines (series 1 and 2) and croconates (series 3). We have applied several criteria to evaluate the diradical character of these

molecules, which include calculation of the singlet–triplet gap and estimation of the diradical character by the occupation numbers in the symmetry broken singlet state. We find a good correlation of the absorption in NIR and diradical character. Then we have systematically studied the absorption properties of these dyes using TD-DFT methods, and we find that one series (3) has on average a large deviation from the experimentally observed values, which we attribute to the larger diradical character. On the other hand, series 1 and 2, where the average diradical character is small, can be reliably studied by combining DFT methods and linear regression approach.

Computational Methodology

The results of the calculations reported in this work have been obtained using the G03w and the ADF software packages.^{13,14} All of the molecules examined in this study are shown in Chart 1. Nineteen molecules of symmetrical squaraines (1–19) and twenty molecules of the unsymmetrical squaraines (20–39) with various substitutions whose experimentally determined absorption maxima are available in the literature have been chosen for series 1 and 2.^{15–23} Not many experimental studies have been reported for the croconate dyes; hence, only 10 molecules (40–49) of these have been chosen for the third series.^{4a,16a,24–26} Long-chain alkyl substitutions have been replaced with smaller alkyl groups, for computational simplicity. This approximation has been found not to have any effect on the absorption energy in earlier studies.⁷

SCHEME 2: Molecular Orbital Correlation Diagram of an Oxyallyl Diradical



The singlet ground state geometries of these molecules have been initially optimized for different conformations at the RB3LYP/6-31G level with symmetry using G03w, and the lowest energy conformation obtained (minima confirmed by frequency calculation) was again fully reoptimized at the RB3LYP/6-311+G(d,p) level. The final geometries reported here have been obtained with the higher basis set, RB3LYP/6-311+G(d,p). To obtain the adiabatic singlet–triplet gap, the lowest triplet state geometries have been calculated at the UB3LYP/6-311+G(d,p) level of theory for the croconates. Default convergence criterion, for both the SCF convergence and for the residual forces on the atom, in optimization of the geometry is employed. For calculation of the vertical excitation energies, the TD–DFT methodology is used. Here we have made use of the two exchange–correlation functionals, B3LYP and BLYP. Only the lowest intense transitions are considered here (oscillator strengths are reported in the Supporting Information).

The minimized singlet geometries obtained above are used as the starting points to carry out the geometry optimization of the singlet states in ADF software using the BLYP exchange correlational functional with the TZP basis and then TD–DFT carried out using the LB94 asymptotic functional with the TZ2P basis set. To obtain the triplet state geometries and energies of the croconates, the UBLYP/TZP level was used. We obtained similar adiabatic singlet –triplet gaps for the croconates at the B3LYP/6-311+G(d,p) and at the BLYP/TZP levels (Supporting Information, Table A). As the BLYP/TZP method is computationally less expensive, we used this for estimation of the singlet–triplet gaps in all the squaraines.

Solvent effects on the excitation energies have been estimated using the polarizable continuum model (PCM) in the G03w software and COSMO in the ADF package.^{27,28} We have used chloroform and DCM as the solvent for most of the cases as reported in the original experiment and ethanol/methanol and DMSO in some cases. As we are dealing with systems that absorb in a wide range from visible to near-infrared, we shall report all values in wavelength (nm) and not energies (eV) for a clearer picture.

Results and Discussions

Geometry. Geometry data obtained by all of the methods are given in the Supporting Information (Tables B–H). To the best of our knowledge, there is no reported experimental data of the bond lengths and bond angles for the unsymmetrical squaraines and croconate molecules, whereas for the

symmetrical squaraines, some crystal structures have been reported in CSD.²⁹ The reliability of the DFT methods in reproducing the experimental geometry of the oxyallyl derivatives has been evaluated earlier; hence, no further discussion of this is carried out here.⁷ However, relative comparisons of the oxyallyl subgroup present in the three dye series is brought out here. It is found that the C=O bond length obtained in squaraine varies from 1.221 to 1.247 Å, whereas in unsymmetrical squaraines, the bond lengths have a slightly larger range, 1.218–1.249 Å. In case of the croconates, there is a lengthening of this bond, and it varies from 1.236 to 1.276 Å. The C–C–C bond angle of the oxyallyl subgroup is around 89–92° in both the types of squaraines but increases to above 107° in croconates. In the triplet geometry, there is a very slight decrease (~0.009 Å) of the C=O bond length and a slight increase of the angle of the C–C–C bond (1–2°), in the croconates.

Diradicaloid Character. The molecular orbital correlation diagram of an oxyallyl molecule is depicted in Scheme 2. On the left side of the diagram is shown the unperturbed trimethylene methane (TMM) system, where the two singly occupied nonbonding orbitals (NBO), ψ_1 and ψ_2 , are degenerate. On the right side of the diagram is shown the perturbed oxyallyl diradical in which the degeneracy is lost in the NBO. HLG is the HOMO–LUMO gap now, which is the difference of energy between the two now nondegenerate NBOs. A diradicaloid (a diradical derivative) is defined as a molecule with an even number of electrons whose simple MO description contains two approximately nonbonding orbitals with two electrons in low-energy electronic states.^{30,31} The squaraines, unsymmetrical squaraines, and croconates can be classified as diradicaloids as per this definition.

To understand the orbital interaction relation to the HLG, we consider only the atomic orbitals Φ_1 and Φ_2 of the nonbonded carbons 1 and 2 for mathematical simplicity. The linear combinations of these form the bonding and the antibonding molecular orbitals. The secular determinant of the two electron–two orbital case is given below³²

$$\begin{vmatrix} E_1^0 - E & \Delta_{12} - ES_{12} \\ \Delta_{12} - ES_{12} & E_2^0 - E \end{vmatrix} = 0$$

where

$$\Delta_{12} = \langle \Phi_1 | H | \Phi_2 \rangle S_{12} = \langle \Phi_1 | \Phi_2 \rangle$$

Here $E_1^0 = E_2^0$ (degenerate due to the symmetry). Hence this leads to solutions

$$E_1' = \frac{E_1^0 + \Delta_{12}}{1 + S_{12}} \quad E_2' = \frac{E_1^0 - \Delta_{12}}{1 - S_{12}}$$

When S_{12} is small

$$E_1' \approx E_1^0 + (\Delta_{12} - E_1^0 S_{12}) - S_{12}(\Delta_{12} - E_1^0 S_{12})$$

$$E_2' \approx E_1^0 - (\Delta_{12} - E_1^0 S_{12}) - S_{12}(\Delta_{12} - E_1^0 S_{12})$$

The HLG can then be written as

$$\text{HLG} = E_2' - E_1' = 2(E_1^0 S_{12} - \Delta_{12}) \quad (1)$$

This clearly shows that, on lowering the interaction between the two orbitals Φ_1 and Φ_2 , there is lowering of the HLG due to the smaller values of S_{12} and Δ_{12} . This can be also brought out qualitatively using the molecular orbitals.^{30b} A decreased interaction in the bonding HOMO destabilizes it, and an increased interaction in the antibonding LUMO stabilizes it, thus lowering the HLG.⁷ At the extreme case of HLG = 0, we get a pure diradical. This lowering of the interaction can initially be achieved by increasing the angle, θ , indicated in Scheme 2. Thus, croconates with a larger angle (above 107°) should have larger diradical character than the squaraines (90°).^{7b} The lowering of the HLG can also be achieved by other perturbations, like substitutions. Molecules with small diradical character can be studied using single determinant methods but much larger diradical character would require multiconfigurational methods to describe it with inclusion of determinants like the one given below on the right side (unnormalized and not spin adapted) to the ground state determinant given on the left.

$$\left| \begin{array}{cc} \Psi_1(1)\alpha(1) & \Psi_1(1)\beta(1) \\ \Psi_1(2)\alpha(2) & \Psi_1(2)\beta(2) \end{array} \right| + \left| \begin{array}{cc} \Psi_2(1)\alpha(1) & \Psi_2(1)\beta(1) \\ \Psi_2(2)\alpha(2) & \Psi_2(2)\beta(2) \end{array} \right|$$

Alternatively, as recently suggested, broken symmetry methods using the unrestricted formalism or the spin flipping can also be utilized.^{33–36} The former method was in fact utilized to carry out the DFT study of the excited singlet oxyallyl molecule, which is a pure diradical (triplet ground state). Hess et al., used the broken symmetry formalism at the B3LYP/6-31G(d) level to obtain the singlet diradical.³⁷ They obtained the stable singlet species with an S^2 value of 0.8.

On the basis of the MO diagram, we can expect a small diradical character in the singlet. There are several criteria to evaluate the singlet diradical nature of these systems.^{33–35} One criterion would be the energy lowering obtained by the symmetry broken DFT solution in the unrestricted formalism, when compared to the energy value obtained at the restricted formalism. In other words

$$E_1 = E_{\text{UDFT}}(\text{singlet}) - E_{\text{RDFT}}(\text{singlet}) \quad (2)$$

To check this, we carried out the calculations in the broken symmetry at each stationary point using the GUESS=mix option for the B3LYP methods. Here this option induces, for the frontier orbitals, symmetry broken guess orbitals by forming the linear combination of the symmetry adapted restricted guess orbitals (both plus and minus combinations). By using these orbitals, we should obtain the symmetry broken solutions. We did not find any energy change with this method when compared to the spin restricted method, and S^2 obtained was zero in all of

TABLE 1: HOMO–LUMO Gap (HLG in eV), E_2 (in kcal/mol), and Diradical Character (Y_0 at UHF) of Symmetrical Squaraines

mol. no.	R	HLG	E_2	Y_0
1	R ₇	2.32	26.9	0.156
2	R ₂	2.33	27.0	0.161
3	R ₅	2.38	29.4	0.032
4	R ₃	2.31	26.6	0.146
5	R ₂₃	2.25	26.1	0.180
6	R ₁₂	1.93	20.0	0.347
7	R ₁₃	1.70	16.9	0.439 ^a
8	R ₁₆	2.44	28.3	0.184
9	R ₁	2.49	28.07	0.199
10	R ₂₆	2.29	26.3	0.175
11	R ₂₄	2.15	25.3	0.232
12	R ₃₃	2.26	24.9	0.102
13	R ₂₅	2.15	23.9	0.217
14	R ₂₂	1.95	21.1	0.136
15	R ₂₉	2.17	24.4	0.096
16	R ₁₈	2.42	30.7	0.000
17	R ₃₆	2.63	33.4	0.007
18	R ₂₇	2.19	25.5	0.018
19	R ₁₀	2.49	29.0	0.207

^a $E_1 = 2.1$ kcal/mol; $Y_0 = 0.068$ obtained at BH and HLYP.

TABLE 2: HOMO–LUMO Gap (HLG in eV), E_2 (in kcal/mol), and Diradical Character (Y_0 at UHF) of Unsymmetrical Squaraines

mol. no.	R	R'	HLG	E_2	Y_0
20	R ₂₈	R ₂₃	1.82	18.7	0.316 ^a
21	R ₃₅	R ₂₃	1.87	20.1	0.348 ^b
22	R ₃₃	R ₁₇	1.93	20.8	0.164
23	R ₃₂	R ₂	2.25	25.9	0.122
24	R ₁₅	R ₅	2.47	28.8	0.090
25	R ₃₄	R ₅	2.64	32.7	0.000
26	R ₁	R ₂₀	2.66	32.6	0.053
27	R ₇	R ₁	2.41	27.4	0.172
28	R ₆	R ₂	2.31	26.4	0.162
29	R ₈	R ₄	2.26	25.7	0.165
30	R ₃₃	R ₁₉	2.32	26.9	0.071
31	R ₁₁	R ₅	2.43	28.5	0.112
32	R ₈	R ₁	2.36	26.9	0.170
33	R ₈	R ₅	2.28	27.2	0.101
34	R ₈	R ₁₁	2.30	26.5	0.201
35	R ₂₉	R ₉	2.65	31.5	0.019
36	R ₁	R ₂	2.41	28.5	0.176
37	R ₁	R ₅	2.51	29.6	0.081
38	R ₂	R ₅	2.38	29.7	0.078
39	R ₂	R ₃	2.32	27.8	0.153

^a $E_1 = 0.4$ kcal/mol, $Y_0 = 0.010$. ^b $E_1 = 0.3$ kcal/mol, $Y_0 = 0.009$; obtained at BH and HLYP.

the cases. It is known from earlier studies that the singlet diradical character should be very large for the broken symmetry unrestricted DFT energy to be lower.^{33a} Very recently, some reports have suggested the usage of BH and HLYP functionals for diradicals; hence, we make use of these here for estimation of the energy E_1 .^{38,39} In most of the squaraines except in 7, 20, and 21 (values shown in Tables 1 and 2 as footnotes), we find the value is close to zero, whereas in the case of 6, 3, and 11, we did not get a proper convergence. In croconates (Table 3) except 42 and 43, all of the molecules show an E_1 value in the range of 2.7–7.5 kcal/mol. The behavior of 42 and 43 shall be discussed later.

Another criterion is the singlet–triplet gap. According to Wirz, to classify a molecule as a diradicaloid, the energy of the singlet–triplet (E_2) splitting should lie around 2–24 kcal/mol.⁴⁰ This is defined as

$$E_2 = E_{\text{UDFT}}(\text{triplet}) - E_{\text{RDFT}}(\text{singlet}) \quad (3)$$

TABLE 3: E_1 (in kcal/mol), E_2 (in kcal/mol), Diradical Character (Y_0), and HOMO–LUMO Gap (HLG in eV) of Croconates

mol. no.	R	E_1	E_2	Y_0^a	Y_0^b	HLG
40	R ₁₂	6.0	10.1	0.602	0.201	1.51
41	R ₁₃	7.5	7.8	0.665	0.269	1.33
42	R ₁₄	0.7	16.1	0.188	0.021	1.77
43	R ₅	0.6	17.1	0.212	0.018	1.79
44	R ₈	3.6	13.7	0.437	0.116	1.75
45	R ₂₁	2.7	14.4	0.347	0.081	1.78
46	R ₂₉	3.0	14.2	0.364	0.094	1.70
47	R ₃₀	3.1	14.0	0.378	0.099	1.69
48	R ₃₁	2.9	14.3	0.358	0.091	1.70
49	R ₂₂	3.5	12.5	0.438	0.117	1.54

^a At UHF. ^b At UBH and HLYP.

We find 6 and 7 have small E_2 values of about 20 and 16.9 kcal/mol, respectively, in the first series (shown in Table 1). Molecule 14 also has a small E_2 gap of 21.1 kcal/mol. All others in this series have large gaps of over 24 kcal/mol. In Table 2, the E_2 values of series 2 are shown. Here 20, 21, and 22 have small gaps, which are in the range of 18–20 kcal/mol. In the third series, shown in Table 3, all of these have very small gaps with the maximum of 17 kcal/mol for 43. The lowest gap is 7.8 kcal/mol obtained for 41. This gives an indication of the larger diradical character in this series. The HLG are also on average lower in this series.

We now estimate the diradical character, Y_0 , by using the unrestricted formalism at the DFT optimized geometries. It is expressed in spin projection theory as^{38,39}

$$Y_i = 1 - \frac{2S_i}{1 + S_i^2} \quad (4)$$

Here S_i is the orbital overlap between the corresponding occupied and unoccupied orbital pairs (HOMO- i and LUMO+ i) and S_i is determined by using the occupation numbers (n_i) of the unrestricted formalism natural orbitals

$$S_i = \frac{n_{\text{HOMO}-i} - n_{\text{LUMO}+i}}{2}$$

The diradical character, Y_0 , is calculated by this equation using the HOMO and LUMO of the UHF natural orbitals and also the DFT methods: UB3LYP, UBLYP, and UBH and HLYP. It is known that the DFT methodologies like UB3LYP and UBLYP underestimate the diradical character, and we found this to be the case with these also, which actually predict zero diradical character.^{38b} The values obtained by UHF, UBH, and HLYP methods are shown in Tables 1 (symmetrical squaraines), 2 (unsymmetrical squaraines), and 3 (croconates). The diradical character varies from 0 to 1, which corresponds to 0% diradical character to 100%. The diradical character in the squaraine series obtained by the UHF is small and almost between 10–20% except in the case of 6 and 7. Here it is found to be between 30 and 40%, which is an intermediate range. The reason for only these two molecules to have large diradical character is attributed to the substitutions which are pyrylium and thiopyrylium, which stabilize the diradical form. In Table 2, we also find 20 and 21 have large diradical character, where again the heteroatoms like oxygen in the side rings stabilize it. It is found that on an average that the croconate series in Table 3 has a larger diradical character, and in 40 and 41, the diradical character is almost 60–70%.

It is seen that 42 and 43 have a smaller diradical character of around 20%. These two molecules are the only ones in the series

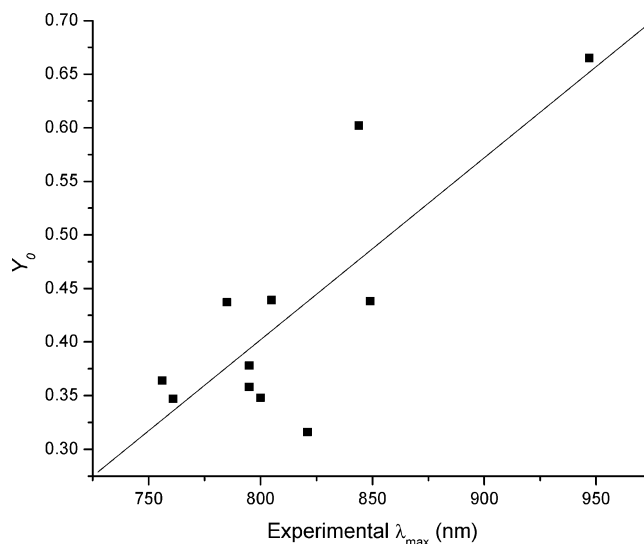


Figure 1. Diradical character versus experimental λ_{max} (nm) for all the molecules absorbing above 750 nm.

with H-bonding and are not connected to the main oxyallyl ring through a conjugated bond. They are in fact directly connected and rotated out of plane. The H-bonding between the oxyallyl oxygen and the OH hydrogens of the side groups stabilizes the ionic character and induces a larger coupling between the diradical form and the mesoionic form.^{7d} Our earlier studies using high level SAC-CI clearly shows that these molecules have a fairly large dipole moment in the ground state which does not change upon excitation.⁷ It should be mentioned that the E_2 values for 42 and 43 molecules are within 20 kcal/mol, indicating some diradical nature.

The values obtained by the UBH and HLYP methods are very small and are clearly underestimated, in agreement with other studies on different molecules.³⁵ To study the effect of geometry, we also optimized 40 in C_2 (original C_s) symmetry and estimated the diradical character. The diradical character almost remains the same.

We now bring out a correlation of the diradical character and the experimental absorption energies. This is shown in Figure 1. Here we only look for the correlation of the NIR absorption, above 750 nm wavelength, and the diradical character obtained by eq 4. In the figure, we do not consider 42 and 43 (vide supra). There is very good near linear relationship indicating that the NIR absorption in these is due to the dominance of the diradical character. All of these have a diradical character of more than 30%. We also observe that the squaraines having the same substitution as the corresponding croconates have lower diradical character and shorter absorption maxima in agreement with eq 1. For 6, the calculated diradical character is 0.347 and absorption is 713 nm, whereas in croconate 40 where the side groups are same (R₁₂) the diradical character is 0.602 and absorption is 845 nm. Another example is squaraine 7 and croconate 41 (side groups R₁₃). Here the diradical character is 0.439 in 7 and absorption is 804 nm, whereas in 41, it is 0.665 and absorption is 950 nm. We have come across only two experimental studies where the comparison of the absorption maxima has been made for squaraines and croconates with similar substitutions.^{16a} Keil et al. have suggested that the stronger auxochromic strength of the croconic acid moiety is the reason for the red shift.²⁴ On the other hand, Simard et al. suggested the narrowing of HLG, as estimated from the oxidation/reduction potentials, as the reason for the red shift.^{16a} In this study, it is clearly brought out in terms of diradical character.

TABLE 4: Effect of Basis Set on λ_{Max} in Vacuo and Solvent Calculated Using the B3LYP Functional

mol no.	Y_0	6-31G(d,p)	6-311G(d,p)	6-311+G(2d,2p)	PCM-6-31G(d,p)	PCM-6-311G(d,p)	PCM-6-311+G(2d,2p)
6	0.347	579	583	583	599	603	603
17	0.007	459	462	472	484	487	498
21	0.348	636	639	639	678	680	679
26	0.005	463	464	468	492	493	497
41	0.665	752	751	746	805	805	797
43	0.212	626	624	631	689	688	694

TABLE 5: Calculated λ_{Max} (in nm) of Symmetrical Squaraines

mol. no.	experimental λ_{Max}	TD-B3LYP/6-311G(d,p)		TD-BLYP/6-311G(d,p)		TD-LB94/TZ2P		ref
		vacuo	solvent	vacuo	solvent	vacuo	solvent	
1	634	528	563	565	593	559	554	15a
2	627	524	554	557	583	554	551	15b
3	636	509	546	538	573	549	551	15b
4	643	533	566	595	595	569	564	15b
5	661	536	575	568	599	566	566	15b
6	713	583	603	610	619	608	566	16a
7	804	640	681	662	672	660	617	16a
8	580	488	511	504	515	504	490	18b
9	536	503	516	541	545	525	498	18c
10	645	531	566	566	595	561	561	15b
11	684	563	600	585	618	596	582	16b
12	633	545	569	581	603	588	569	16c
13	663	548	583	569	593	569	559	17a
14	732	617	643	681	689	678	633	17b
15	667	575	601	614	631	605	577	17b
16	651	500	544	530	580	556	564	17c
17	562	462	487	482	508	500	492	18a
18	663	567	596	602	629	642	629	18a
19	544	471	492	471	503	486	463	18b

TABLE 6: Calculated λ_{Max} (in nm) of Unsymmetrical Squaraines

mol. no.	experimental λ_{Max}	TD-B3LYP/6-311G(d,p)		TD-BLYP/6-311G(d,p)		TD-LB94/TZ2P		ref
		vacuo	solvent	vacuo	solvent	vacuo	solvent	
20	821	656	706	707	757	656	701	19a
21	800	639	680	690	726	689	678	19a
22	683	613	640	660	673	660	629	22b
23	624	555	590	598	629	593	577	20a
24	562	504	527	547	572	546	534	20b
25	569	484	510	521	547	534	528	19b
26	484	464	493	489	520	506	502	20c
27	584	513	536	552	564	539	521	21a
28	632	531	562	569	588	564	554	21a
29	622	536	563	570	588	564	554	21b
30	608	527	553	562	582	566	551	21c
31	600	492	523	514	543	521	519	21b
32	564	519	534	555	561	539	515	21b
33	643	521	558	547	574	551	546	21b
34	612	510	539	528	548	530	515	21b
35	514	484	495	519	525	523	502	23
36	578	512	533	550	562	537	519	20b
37	563	493	518	528	549	530	517	20b
38	626	512	550	544	580	551	551	22a
39	632	526	565	563	587	561	554	22a

Vertical Excitations. To study the effect of basis sets on vertical transitions, we first picked up two molecules from each set (one with large diradical character and other small) and carried out studies using the B3LYP functional both in vacuo and in solvent by adding diffuse functions (Table 4). From the table, it is clearly seen that the solvent effects are more important and a difference of 30–50 nm shift is seen with the inclusion of solvent, whereas the effect of adding diffuse functions shifts the absorption to the maximum by only 11 nm. Keeping in view the computational time, we carried out all of our calculations at the 6-311G(d,p) level with and without the solvent. Vertical transition energies calculated by TD-DFT using the B3LYP/BLYP functional with the 6-311G(d,p) basis set on the

geometries obtained at the B3LYP/6-311+g(d,p) level is shown in Table 5 for squaraines, Table 6 for unsymmetrical squaraines, and Table 7 for croconates. Shown in the same tables are the vertical transition energies obtained at the LB94/TZ2P level at the BLYP/TZP geometries. We first discuss results obtained for series 1 and 2. In series 1, the minimum deviation in B3LYP is seen to be around 33 nm, whereas the maximum is 164 nm. In the molecules with larger diradical character in these series, namely 6, 7, 20, and 21, we notice that the deviation is the maximum in their respective series. In the case of BLYP, the deviations are in the range of 5–142 nm. In the LB94 also the deviation is not much different; the range is between 11–144 nm. Inclusion of the solvent effect in these two series, using

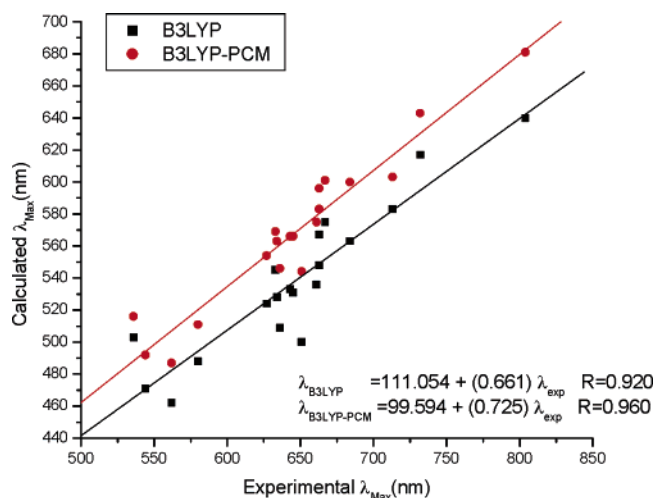


Figure 2. Calculated versus experimental λ_{max} (nm) of symmetrical squaraines at the B3LYP/PCM-B3LYP/6-311G(d, p) level.

B3LYP/BLYP, brings out a better agreement with the experimental values (Tables 5 and 6). The average deviation in B3LYP without solvent is 108.2, whereas with solvent, it is 78 nm. In the case of BLYP, the average deviation is 77.2, whereas with solvent, it is 55.4, and in the case of LB94, the average deviation is 73.9, whereas with solvent, it is 89.1 nm. In series 2, the range of deviation in the B3LYP case is 20–165 nm, whereas again in BLYP, there is a decrease in the range of deviation to 5–114 nm and, in LB94, 9–165 nm. The average deviation in B3LYP without solvent is 86.5, whereas with solvent, it is 58.2. In the case of BLYP, the average deviation is 51.4, whereas with solvent, it is 33.5, and in the case of LB94, the average deviation is 56.2, whereas with solvent, it is 64.7 nm. The deviations, in the case of B3LYP and BLYP, with inclusion of solvent is reduced, but on the other hand, inclusion of the solvent effects in the case of the LB94 functional show a slightly larger deviation from the experiment values.

The least-squares fit of the λ_{max} of the squaraines for the B3LYP/6-311G(d, p) level is carried out, both with and without solvent effects, and is shown in Figures 2 and 3. We obtain a good fit, and the R value is above 0.90. Thus, the errors in these series turn out to be systematic which can be attributed to the inherent approximations in the TD-DFT.^{9a} On the other hand, LB94 with and without solvent does not perform as well as the other functionals for the symmetrical squaraines ($R = 0.888$ in vacuo and $R = 0.865$ in solvent), whereas for the unsymmetrical squaraines ($R = 0.895$ in vacuo and $R = 0.944$ in solvent), the correlation is better. The least-square fits of BLYP and LB94

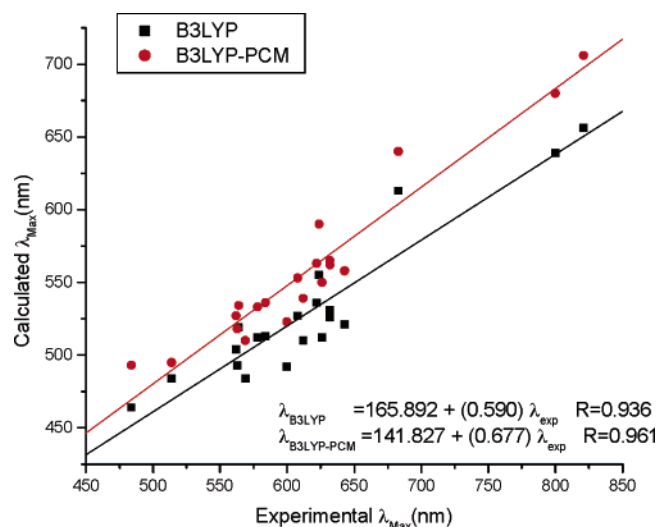


Figure 3. Calculated versus experimental λ_{max} (nm) of unsymmetrical squaraines at the B3LYP/PCM-B3LYP/6-311G(d, p) level.

with and without solvent are given in the Supporting Information (Figures A and B).

Table 7 for croconates reveals that the deviations are as large as 250 nm, and the solvent inclusion decreases it a bit. There is no improvement even with the BH and HLYP functional (carried out only in this case) as seen in the same tables. Overall, the average deviations here are larger and between 64–201 nm. More interestingly, the least-square fit does not give any reasonable R value suggesting that the deviations are not systematic (scatter plot shown in Figure 4 only for B3LYP, whereas the scatter plots for other functionals are shown in the Supporting Information, Figure C). We carried out further calculations on molecule 41 to study the effect of basis sets (addition of diffuse functions) and functionals, and this is shown in Table 8. It is seen that average deviation for this molecule is still greater than 100 nm, in all of the methods. We infer from this that the deviation from the experimental values is not due to the inherent approximations in the TD-DFT methodologies but due to the greater number of molecules with larger diradical character in the croconate series. This leads us to conclude that the single reference DFT methods may not be applicable for these croconate molecules.

Conclusions

Evaluation of the diradical character of the oxyallyl derivatives using the DFT methods with broken symmetry formalism reveals that it is underestimated. On the other hand, the UHF natural orbitals are a good choice to estimate this character. The

TABLE 7: Calculated λ_{Max} (in nm) of Croconates

mol. no.	experimental λ_{Max}	TD-B3LYP/6-311G(d,p)		TD-BLYP/6-311G(d,p)		TD-BHandHLYP/6-311G(d,p)		TD-LB94/TZ2P		ref
		vacuo	solvent	vacuo	solvent	vacuo	solvent	vacuo	solvent	
40	845	689	721	709	723	684	740	697	653	16a
41	950	751	805	757	786	753	840	752	701	16a
42	880	621	693	647	718	601	679	689	713	4
43	817	624	688	668	706	601	677	649	667	24
44	786	622	674	630	653	620	690	639	639	24
45	759, 799 ^a	641	679	662	701	624	666	678	689	25, 26c ^a
46	771, 798 ^a	678	707	694	703	664	706	693	685	26b, 26c ^a
47	794	686	729	694	743	670	730	709	685	26a
48	795	687	733	707	752	667	730	705	697	26a
49	847	712	749	745	779	696	756	738	685	26a

^a Values from reference 26c, but the solvent used was not reported.

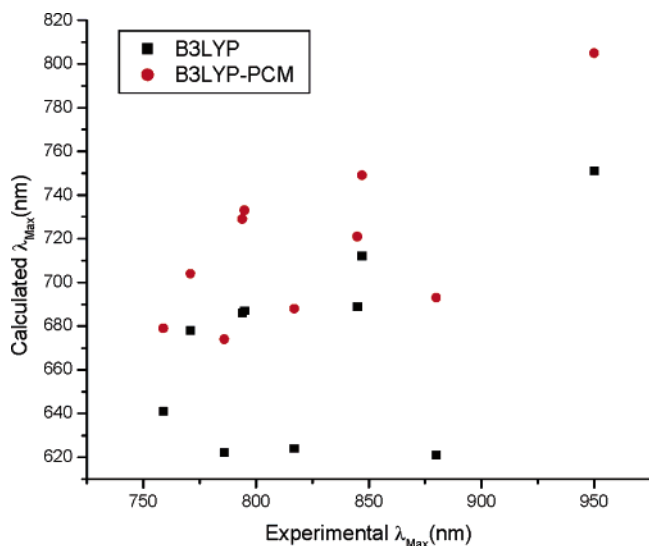


Figure 4. Calculated versus experimental λ_{max} (nm) of croconates at the B3LYP/PCM-B3LYP/6-311G(d,p) level.

TABLE 8: Calculated λ_{Max} (in nm) for Croconate 41 Using Different Basis Sets and Functionals

functional	6-31G(d,p)		6-311G(d,p)		6-311+G(2d,2p)	
	vacuo	solvent	vacuo	solvent	vacuo	solvent
B3LYP	752	806	751	805	746	797
BLYP	775	807	757	786	728	783
O3LYP	756	802	755	802	749	793
PBE0	770	804	761	791	717	760
BHandHLYP	754	842	753	840	747	829
mPW1PW91	770	804	751	764	719	755

adiabatic singlet triplet gap calculated by the DFT methods is in good agreement with the estimated diradical character by the UHF natural orbitals. A very good correlation of the diradical character above 35% and the NIR absorption has been brought out for the oxyallyl derivatives. The longer wavelength absorption in the croconates compared to the squaraines is clearly due to the larger diradical nature in the former. The diradical nature in most of the squaraines is small, so that the energy of absorption of symmetrical squaraines and unsymmetrical squaraines can be calculated with reasonable accuracy using a medium size basis set in TD-DFT + linear scaling methods. The linear regression analysis of the symmetrical squaraine series using the PCM-B3LYP/6-311G(d,p) values is

$$\lambda_{\text{PCM-B3LYP}} = 99.594 + (0.725\lambda_{\text{EXP}})$$

with an R value of 0.960, whereas for the unsymmetrical squaraines at the same level it is

$$\lambda_{\text{PCM-B3LYP}} = 141.827 + (0.677\lambda_{\text{EXP}})$$

with an R value of 0.961. Using this equation, the average deviation with experiment is reduced in these series. As the DFT is a single determinant theory when the average diradical character of the molecules in a series is large, the deviation from the experiment on average is large as seen in series 3, croconates. Thus, for these systems, a multiconfigurational wave function may be needed for the description.

Acknowledgment. The authors thank DST, New Delhi for the funding of this project. The authors also thank The Director, ICT, and The Head, Inorganic Chemistry Division, for their constant support and encouragement of this work. Ch.P. thanks

DST for the fellowship, and K.S., C.L.D., and K.Y. thank CSIR for the fellowship.

Supporting Information Available: Geometry data obtained by all of the methods. This material is available free of charge via the Internet at <http://pubs.acs.org>.

References and Notes

- (1) (a) Fabian, J. *Chem. Rev.* **1992**, *92*, 1197. (b) Fabian, J.; Zahradnik, R. *Angew. Chem. Int. Ed.* **1989**, *28*, 677.
- (2) (a) Mustroph, H.; Stollenwerk, M.; Bressau, V. *Angew. Chem. Int. Ed.* **2006**, *45*, 2016. (b) Law, K. Y. *Chem. Rev.* **1993**, *93*, 449.
- (3) (a) *IR Absorbing Dyes*; Matsuoka, M., Ed.; Plenum Press: New York, 1990. (b) *Near-Infrared Dyes for High Technology Applications*; Daehne, S.; Resch-Genger, U.; Wolfbeis, O. S., Eds.; NATO ASI Series 3; Kluwer Academic: Dordrecht, The Netherlands, 1998; Vol. 52.
- (4) Tian, M.; Tatsuura, S.; Furuki, M.; Sato, Y.; Iwasa, I.; Pu, L. S. *J. Am. Chem. Soc.* **2003**, *125*, 348.
- (5) (a) Tatsuura, S.; Tian, M.; Furuki, M.; Sato, Y.; Iwasa, I.; Mitsu, H. *Appl. Phys. Lett.* **2004**, *84*, 1450. (b) Tatsuura, S.; Mastubara, T.; Tian, M.; Mitsu, H.; Iwasa, I.; Sato, Y.; Furuki, M. *Appl. Phys. Lett.* **2004**, *85*, 540. (c) Avlasevich, Y.; Mullen, K. *Chem. Commun.* **2006**, 4440.
- (6) (a) Meier, H.; Petermann, R. *Helv. Chim. Acta* **2004**, *87*, 1109. (b) Ajaya Ghosh, A. *Acc. Chem. Res.* **2005**, *38*, 449. (c) Meier, H.; Dullweber, U.; *Tetrahedron Lett.* **1996**, *37*, 1191. (d) Langhals, H. *Angew. Chem. Int. Ed.* **2003**, *42*, 4286.
- (7) (a) Prabhakar, Ch.; Krishna Chaitanya, G.; Sitha, S.; Bhanuprakash, K.; Jayathriha Rao, V. *J. Phys. Chem. A* **2005**, *109*, 2614. (b) Prabhakar, Ch.; Yesudas, K.; Krishna Chaitanya, G.; Sitha, S.; Bhanuprakash, K.; Jayathriha Rao, V. *J. Phys. Chem. A* **2005**, *109*, 8604. (c) Yesudas, K.; Krishna Chaitanya, G.; Prabhakar, Ch.; Bhanuprakash, K.; Jayathriha Rao, V. *J. Phys. Chem. A* **2006**, *110*, 11717. (d) Yesudas, K.; Bhanuprakash, K. *J. Phys. Chem. A* **2007**, *111*, 1943.
- (8) Fabian, J. *Theor. Chem. Acc.* **2001**, *106*, 199.
- (9) (a) Champagne, B.; Guillaume, M.; Zutterman, F. *Chem. Phys. Lett.* **2006**, *425*, 105. (b) Jacquemin, D.; Perpète, E. A. *Chem. Phys. Lett.* **2006**, *420*, 529. (c) Guillaume, D.; Nakamura, S. *Dyes Pigm.* **2000**, *46*, 85. (d) Fratiloiu, S.; Candeias, L. P.; Grozema, F. C.; Wildeman, J.; Siebbeles, L. D. A. *J. Phys. Chem. B* **2004**, *108*, 19967.
- (10) (a) Preat, J.; Jacquemin, D.; Wathelet, V.; André, J.; Perpète, E. A. *J. Phys. Chem. A* **2006**, *110*, 8144. (b) Jacquemin, D.; Preat, J.; Wathelet, V.; Fontaine, M.; Perpète, E. A. *J. Am. Chem. Soc.* **2006**, *128*, 2072.
- (11) (a) Jacquemin, D.; Perpète, E. A. *Chem. Phys. Lett.* **2006**, *429*, 147. (b) Jacquemin, D.; Preat, J.; Wathelet, V.; Perpète, E. A. *J. Chem. Phys.* **2006**, *124*, 074104.
- (12) (a) Wathelet, V.; Preat, J.; Bouhy, M.; Fontaine, M.; Perpète, E. A.; Andre, J.-M.; Jacquemin, D. *Int. J. Quantum. Chem.* **2006**, *106*, 1853. (b) Jacquemin, D.; Bouhy, M.; Perpète, E. A. *J. Chem. Phys.* **2006**, *124*, 204321.
- (13) Frisch, M. J.; Trucks, G. W.; Schlegel, H. B.; Scuseria, G. E.; Robb, M. A.; Cheeseman, J. R.; Montgomery, Jr. J. A.; Vreven, T.; Kudin, K. N.; Burant, J. C.; Millam, J. M.; Iyengar, S. S.; Tomasi, J.; Barone, V.; Mennucci, B.; Cossi, M.; Scalmani, G.; Rega, N.; Petersson, G. A.; Nakatsuji, H.; Hada, M.; Ehara, M.; Toyota, K.; Fukuda, R.; Hasegawa, J.; Ishida, M.; Nakajima, T.; Honda, Y.; Kitao, O.; Nakai, H.; Klene, M.; Li, X.; Knox, J. E.; Hratchian, H. P.; Cross, J. B.; Adamo, C.; Jaramillo, J.; Gomperts, R.; Stratmann, R. E.; Yazyev, O.; Austin, A. J.; Cammi, R.; Pomelli, C.; Ochterski, J. W.; Ayala, P. Y.; Morokuma, K.; Voth, G. A.; Salvador, P.; Dannenberg, J. J.; Zakrzewski, V. G.; Dapprich, S.; Daniels, A. D.; Strain, M. C.; Farkas, O.; Malick, D. K.; Rabuck, A. D.; Raghavachari, K.; Foresman, J. B.; Ortiz, J. V.; Cui, Q.; Baboul, A. G.; Clifford, S.; Cioslowski, J.; Stefanov, B. B.; Liu, G.; Liashenko, A.; Piskorz, P.; Komaromi, I.; Martin, R. L.; Fox, D. J.; Keith, T.; Al-Laham, M. A.; Peng, C. Y.; Nanayakkara, A.; Challacombe, M.; Gill, P. M. W.; Johnson, B.; Chen, W.; Wong, M. W.; Gonzalez, C.; Pople, J. A. *Gaussian 03*, revision B.01; Gaussian, Inc.: Wallingford CT, 2004.
- (14) (a) Theoretical Chemistry, Vrije Universiteit, Amsterdam, The Netherlands, <http://www.scm.com>. (b) te Velde, G.; Bickelhaupt, F. M.; Baerends, E. J.; Guerra, C. F.; van Gisbergen, S. J. A.; Snijders, J. G.; Ziegler, T. *J. Comput. Chem.* **2001**, *22*, 931.
- (15) (a) Law, K. Y.; Bailey, F. C. *Dyes Pigm.* **1993**, *21*, 1. (b) Law, K. Y. *J. Phys. Chem.* **1987**, *91*, 5184.
- (16) (a) Simard, T. P.; Yu, J. H.; Zebrowski-Young, J. M.; Haley, N. F.; Detty, M. R. *J. Org. Chem.* **2000**, *65*, 2236. (b) Beverina, L.; Abbotto, A.; Landenna, M.; Cerminara, M.; Tubino, R.; Meinardi, F.; Bradamante, S.; Pagani, G. A. *Org. Lett.* **2005**, *7*, 4257. (c) Terpetschnig, E. A. U.S. Patent, 6,538,129 B1, 2003.
- (17) (a) Keil, D.; Hartmann, H.; Moschny, T. *Dyes Pigm.* **1991**, *17*, 19. (b) Kuramoto, K.; Natsukawa, K.; Asao, K. *Dyes Pigm.* **1989**, *11*, 21. (c) Wallace, K. J.; Gray, M.; Zhong, Z.; Lynch, V. M.; Anslyn, E. V. *Dalton Trans.* **2005**, 2436.

- (18) (a) Griffiths, J.; Mama, J. *Dyes Pigm.* **2000**, *44*, 9. (b) Ashwell, G. J.; Handa, T.; Leeson, P.; Skjonnemand, K.; Jefferies, G.; Green, A. *J. Mater. Chem.* **1998**, *8*, 377. (c) Farnum, G. D.; Webster, B.; Wolf, A. D. *Tetrahedron Lett.* **1968**, 5003.
- (19) (a) Yagi, S.; Hyodo, Y.; Matsumoto, S.; Takahashi, N.; Kono, H.; Nakazumi, H. *J. Chem. Soc. Perkin Trans. 1* **2000**, 599. (b) Shimizu, I.; Toyoda, H.; Kinugasa, M.; Yamada, S.; Ikuta, M.; Mutoh, K.; Satoh, T.; Tomura, T. Eur. Patent 1,152,037 A9, 2001.
- (20) (a) Alex, S.; Santhosh, U.; Das, S. *J. Photochem. Photobiol. A: Chem.* **2005**, *72*, 63. (b) Law, K. Y. *J. Org. Chem.* **1992**, *57*, 3278. (c) Marder, S. R.; Chen, C.-T. U.S. Patent 5,500,156, 1996.
- (21) (a) Law, K. Y.; Bailey, F. C. *Dyes Pigm.* **1993**, *21*, 1. (b) Keil, D.; Hartmann, H. *Dyes Pigm.* **2001**, *49*, 161. (c) Tatarets, A. L.; Fedyunyaeva, I. A.; Terpetschnig, E.; Patsenker, L. D. *Dyes Pigm.* **2005**, *64*, 125.
- (22) (a) Law, K. Y.; Bailey, F. C. *J. Chem. Soc. Chem. Commun.* **1991**, 1156. (b) Kim, S.-H.; Hwang, S.-H.; Kim, N.-K.; Kim, J.-W.; Yoon, C.-M.; Keum, S.-R. *J. Soc. Dyers Colour.* **2000**, *116*, 127.
- (23) West, R. M.; Cummins, W. J.; Nairne, R. J.; Domett, B.; Graham, M. CA Patent, 2,366,263, 2001.
- (24) Keil, D.; Hartmann, H.; Reichardt, C. *Liebigs Ann. Chem.* **1993**, 935.
- (25) Encinas, C.; Otazo, E.; Rivera, L.; Miltsov, S.; Alonso, J. *Tetrahedron Lett.* **2002**, *43*, 8391.
- (26) (a) Rillaers, G. A.; Kontich.; Depoorter. U.S. Patent, 3,793,313, 1974. (b) Shigeo, Y.; Masaru, K.; Teijiro, K. *Dyes Pigm.* **1988**, *10*, 13. (c) Miura, K.; Ozawa, T.; Iwanami, J. Japanese Patent 61034092A, 1986.
- (27) (a) Cancès, M. T.; Mennucci, B.; Tomasi, J. *J. Chem. Phys.* **1997**, *107*, 3032. (b) Cossi, M.; Barone, V.; Mennucci, B.; Tomasi, J. *J. Chem. Phys. Lett.* **1998**, *286*, 253. (c) Mennucci, B.; Tomasi, J. *J. Chem. Phys.* **1997**, *106*, 5151.
- (28) Pye, C. C.; Ziegler, T. *Theor. Chem. Acc.* **1999**, *101*, 396.
- (29) Cambridge Crystallographic Data Center (CCSD). 12 Union Road, Cambridge CB2 1EZ, England.
- (30) (a) Michl, J.; Bonacic-Koutecky, V. *Tetrahedron*, **1988**, *44*, 7559. (b) Ichimura, A. S.; Lahti, P. M.; Matlin, A. R. *J. Am. Chem. Soc.* **1990**, *112*, 2868.
- (31) (a) Dohnert, D.; Koutecky, J. *J. Am. Chem. Soc.* **1980**, *102*, 1789. (b) Salem, L.; Rowland, C. *Angew. Chem. Int. Ed.* **1972**, *11*, 92.
- (32) Albright, T. A.; Burdett, J. K.; Whangbo, M.-H. *Orbital Interactions in Chemistry*; Wiley: New York, 1985.
- (33) (a) Bachler, V.; Olbrich, G.; Neese, F.; Wieghardt, K. *Inorg. Chem.* **2002**, *41*, 4179. (b) Adamo, C.; Barone, V.; Bencini, A.; Totti, F.; Ciofini, I. *Inorg. Chem.* **1999**, *38*, 1996.
- (34) (a) Makano, M.; Kubo, T.; Kamada, K.; Ohta, K.; Kishi, R.; Ohta, S.; Nakagawa, N.; Takahashi, H.; Furukawa, S.; Morita, Y.; Nakasuji, K.; Yamaguchi, K.; *Chem. Phys. Lett.* **2006**, *418*, 142. (b) Champagne, B.; Botek, E.; Quinet, O.; Nakano, M.; Kishi, R.; Nitta, T.; Yamaguchi, K. *Chem. Phys. Lett.* **2005**, *407*, 372.
- (35) (a) Nakano, M.; Nitta, T.; Yamaguchi, K.; Champagne, B.; Botek, E. *J. Phys. Chem. A* **2004**, *108*, 4105. (b) Nakano, M.; Kishi, R.; Nitta, T.; Kubo, T.; Nakasuji, K.; Kamada, K.; Ohta, K.; Champagne, B.; Botek, E.; Yamaguchi, K. *J. Phys. Chem. A* **2005**, *109*, 885.
- (36) (a) Champagne, B.; Botek, E.; Nakano, M.; Nitta, T.; Yamaguchi, K. *J. Chem. Phys.* **2005**, *122*, 114315. (b) Krylov, A. I. *Acc. Chem. Res.* **2006**, *39*, 83.
- (37) Hess, B. A., Jr.; Smentek, L. *Eur. J. Org. Chem.* **1999**, 3363.
- (38) Nakano, M.; Kishi, R.; Nakagawa, N.; Ohta, S.; Takahashi, H.; Furukawa, S.; Kamada, K.; Ohta, K.; Champagne, B.; Botek, E.; Yamada, S.; Yamaguchi, K. *J. Phys. Chem. A* **2006**, *110*, 4238.
- (39) Nakano, M.; Kishi, R.; Ohta, S.; Takebe, A.; Takahashi, H.; Furukawa, S.; Kubo, T.; Morita, Y.; Nakasuji, K.; Yamaguchi, K.; Kamada, K.; Ohta, K.; Champagne, B.; Botek, E. *J. Chem. Phys.* **2006**, *125*, 074113.
- (40) Wirz, J. *Pure Appl. Chem.* **1984**, *56*, 1289.